JOURNAL OF AIRCRAFT
Vol. 35, No. 5, September–October 1998

Aeroelastic Stability Investigation of a Composite Hingeless Rotor in Hover

Anita L. Tracy* and Inderjit Chopra†
University of Maryland, College Park, Maryland 20742

The aeroelastic stability of a composite hingeless rotor with elastic couplings is investigated in hover. A two-bladed, Froude-scaled, soft in-plane hingeless rotor model with various isotropic and graphite/epoxy composite flexures was designed and then tested on a hover stand. The rotor with an isotropic flexure was tested first to examine the experimental procedures. The effects of elastic flapwise bending-torsion and chordwise bending-torsion structural coupling on the aeroelastic stability were then investigated using elastically coupled composite flexures. Lag-mode stability test results are compared with the theoretical predictions obtained using the comprehensive aeroelastic rotor analysis, UMARC (University of Maryland Advanced Rotorcraft Code). The introduction of negative chordwise bending-torsion coupling has a stabilizing effect on the lag damping for positive collective pitch angles. Predictions agree with measured data.

Introduction

COMPOSITE materials are widely used in the design of helicopter rotor blades because of their higher strength-to-weight and stiffness-to-weight ratios, superior fatigue characteristics, and better damage tolerance compared to metals. With the application of composite materials, advanced rotor systems such as hingeless and bearingless rotors are becoming feasible today. These advanced design configurations offer mechanical simplicity (fewer parts), more control power, and better maintainability. Because of blade stress and vibration considerations, these rotors are typically designed as soft in-plane rotors, thus making them susceptible to aeroelastic instabilities. To improve the stability of the system, external lag dampers are routinely used. However, small displacements near the root of hingeless rotor systems reduce the effectiveness of these mechanical dampers. These external dampers also increase the mechanical complexity and the procurement and maintenance costs.

The tailorability of composite materials can be used to achieve beneficial structural couplings such as bending-torsion and extension-torsion. These couplings arise from the anisotropic or directional nature of fibrous composites. The utilization of designs exhibiting these couplings offers the potential for improving the blade dynamics and thus eliminating the need for external dampers. Several researchers have shown analytically that these couplings can improve the stability and vibration characteristics of advanced rotor systems.[1–9] However, these composite-tailoring techniques are not exploited by the rotorcraft industry at this time. One possible reason for this is the absence of experimental validation of the analytical predictions obtained by researchers. The objective of this research is to experimentally investigate the influence of elastic couplings on the dynamic behavior of a composite hingeless rotor.

Presented as Paper 96-1597 at the AIAA/ASME/ASCE/AHS/ASC Structures, Structural Dynamics, and Materials Conference, Salt Lake City, UT, April 15–17, 1996; received Nov. 28, 1996; revision received Jan. 2, 1998; accepted for publication March 10, 1998.

*Rotorcraft Fellow, Alfred Gessow Rotorcraft Center; currently Senior Engineer, Pratt & Whitney Aircraft, West Palm Beach, FL 33410. Member AIAA.

†Professor and Director, Alfred Gessow Rotorcraft Center, Department of Aerospace Engineering. Fellow AIAA.

A number of analytical investigations have been undertaken to address the impact of composites on blade aeroelastic stability. Hong and Chopra[1] formulated an aeroelastic stability analysis for a hingeless rotor system in hover using a simple composite-beam analysis. They showed that bending-torsion and extension-torsion couplings can have a powerful influence on blade dynamics. Panda and Chopra[2] extended this analysis to forward flight and demonstrated the potential for increased aeroelastic stability and reduced blade vibration with composite couplings. These simple blade analyses, however, neglected the influence of nonclassical effects such as transverse shear and constrained warping. Smith and Chopra[3,4] developed an improved formulation to examine the dynamics of a hingeless rotor by including a refined modeling of cross-sectional warping, transverse shear, and in-plane ply elasticity. The results showed that nonclassical structural effects are important for blade analysis and composite couplings improved the aeroelastic stability for a composite hingeless rotor. Tracy and Chopra[5,6] further refined this analysis by including the modeling of warping restraint important for open-section beams.

Yuan et al.[7] developed an analysis using a 23-degree-of-freedom element to investigate the aeroelastic stability of composite blades with straight and swept tips. Composite couplings were shown to have substantial influence on hover aeroelastic stability. Fulton and Hodges[8,9] analyzed the hover stability of a hingeless rotor with extension-torsion- and bending-torsion coupled blades. The analysis placed no restrictions upon the magnitudes of displacement and rotations. These couplings were again shown to have a noticeable affect on the behavior of rotor blades. To verify the accuracy of these analytical models, it is important to correlate predictions with experimental data.

There have been several experimental investigations on the aeroelastic and aeromechanical stability of isotropic hingeless rotors.[10–16] Bousman and co-workers[10–12] investigated the behavior of several different rotor configurations with kinematic couplings. The most interesting configuration involved a combination of pitch-lag coupling and structural flap-lag coupling. The addition of negative pitch-lag coupling alone was shown to increase the lead-lag damping of the experimental rotor compared to the baseline case but was not able to stabilize the unstable region. The combined effect of both negative pitch-lag coupling and flap-lag coupling provided some additional damping in the unstable region compared to the pitch-lag coupled configuration alone. Yeager et al.[13] obtained aeromechanical stability data for a soft in-plane hingeless rotor in hover

and forward flight. The investigation examined the influence of blade sweep, droop, and precone, as well as blade pitch-flap coupling. McNulty[14] investigated the flap-lag stability of an isolated rotor in hover and forward flight. The three-bladed soft in-plane hingeless rotor was operated in an untrimmed state (no cyclic pitch and unrestricted cyclic flapping) in the wind tunnel. By keeping the first torsion mode frequency as high as possible, the influence of the torsional degree of freedom was minimized. Sharpe[15] experimentally investigated the importance of including torsional flexibility in addition to coupling between flap and lag bending on a stiff in-plane hingeless rotor in hover. Maier et al.[16] investigated a soft in-plane isolated rotor in hover and forward flight at representative tip speeds. Stability data were collected for a variety of flight conditions and showed clear trends because of the influence of collective pitch in hover and shaft angle and collective pitch in forward flight. All of these investigations were on hingeless rotors with conventional isotropic blades.[10–16] Stability testing of hingeless rotors with composite couplings has not yet been performed.

The objectives of the present research are as follows:

1) Carry out systematic hover tests for aeroelastic stability of a two-bladed, 6-ft-diam, Froude-scaled composite hingeless rotor model with different elastic couplings (chordwise bending-torsion and flapwise bending-torsion coupling).

2) Compare the measured lag mode damping with the theoretical predictions obtained from UMARC (University of Maryland Advanced Rotorcraft Code).

Experimental Model

Model Description

For the experimental investigation, a four-bladed, 6-ft-diam, Froude-scaled hingeless rotor model was designed and built. Figure 1 shows a schematic of a single blade. The main blades were manufactured with a single glass/epoxy spar, a two-ply ±45-deg fiberglass skin, foam core, and tantalum weights. Each blade was designed to have its c.g. and elastic axis near the quarter-chord and to be very stiff relative to the flexbeams. The rotor hub and blades were mounted on a rigid test stand, powered by a variable-speed, water-cooled 2.5-hp-dc motor. For stability measurement, the blades were excited by oscillating the swashplate with servoactuators.

Flexure Design and Fabrication

The structural couplings were introduced through carefully designed flexures. The dimensions were chosen to obtain flap and lag frequencies representative of a typical soft in-plane hingeless rotor blade. The cross-sectional dimensions of the different flexbeam configurations investigated are shown in Fig. 2. The rectangular section shown in Fig. 2a is manufactured from the engineering plastic Torlon®. Figure 2b represents the geometry for a flapwise bending-torsion configuration. The fiber direction of the laminate is indicated by the angled lines in Fig. 2. The final beam shown in Fig. 2c represents the cross section that is of main interest to this study, the chordwise bending-torsion-coupled configuration. As seen in Fig. 2c, the fiber direction is oriented perpendicular to the chordwise axis.

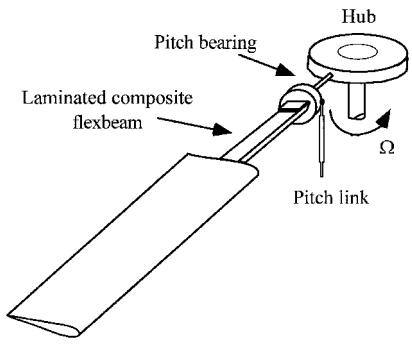

Fig. 1 Schematic of model rotor blade.

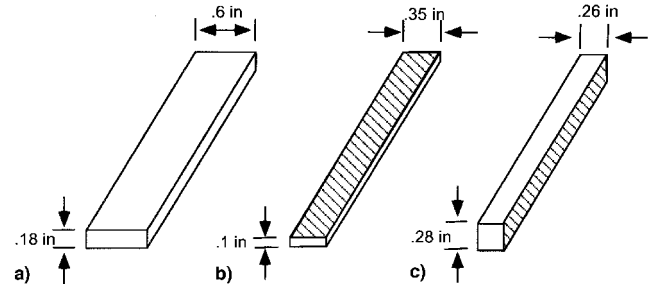

Fig. 2 Cross-sectional dimensions of flexbeams: a) isotropic Torlon section, b) flapwise bending-torsion-coupled section, and c) chordwise bending-torsion-coupled section.

To investigate the effects of flapwise and lagwise bending-torsion coupling, the flexures were designed using unidirectional graphite/epoxy prepreg. The composite flexures were carefully designed to match the natural frequencies of the isotropic rotor as well as to have the desired elastic couplings. An iterative process was used to determine the best combination of ply layup and geometric dimensions to achieve the desired frequencies and stay within the material stress limits. Three different composite flexures were designed, each with different couplings, but with nearly the same fundamental frequencies.

The composite flexures were built out of AS4/3501-6 graphite/epoxy prepreg and cured using an autoclave molding technique. The manufacturing process for the two different cross-sectional geometries varied in its complexity. The material properties and stacking sequences for both types of composite flexures are summarized as follows and in Table 1. Material properties of flexures: Longitudinal modulus E_L = 20.59 msi, transverse modulus E_T = 1.42 msi, shear modulus G_{LT} = 0.89 msi, major Poisson's ratio ν_{LT} = 0.42, ply thickness = 0.005 in. A positive angle is defined as a counterclockwise rotation as seen from the top for a horizontal laminate and from the right for a vertical laminate.

Test Procedures and Data Analysis

Prior to hover testing, nonrotating vibration tests were performed for each configuration to determine modal frequencies and lead-lag structural damping. Blade motion was excited using a sinusoidal swashplate oscillation without the rotor spinning. A frequency sweep approach was used to identify the modes of interest. Once a mode was identified, the value of the natural frequency for that mode was more accurately determined using a narrowband frequency sweep. Once the frequencies were obtained, the next step was to determine the structural lag damping. This was done by using the shake and decay method. The blades were sinusoidally excited at the fundamental lag frequency. After a sufficient level of excitation was evident (typically after about 1 s) the excitation was terminated and the transient response was measured.

Once the nonrotating tests were completed, the rotor was ready to spin. For testing purposes, the model rotor speed was varied up to and including a nominal value of 800 rpm. Prior to data acquisition the rotor was first tracked and trimmed at each rotor speed by adjusting the longitudinal and lateral cyclic pitch to minimize first harmonic flapping. Rotating tests were then performed to determine the rotating natural frequencies and the lag-mode damping. Most configurations were tested at speeds of 0, 600, and 800 rpm, although the bulk of the data was obtained at 600 rpm.

After the rotor was brought up to speed, the first step was to determine the flap, lag, and torsion frequencies. The swashplate was excited through a range of regressing frequencies. Once the desired mode was identified, a narrowband sweep was performed to pinpoint the frequency value. After deter-

Table 1 Stacking sequence of flexures

Configuration	Flapwise bending-torsion coupling	Chordwise bending-torsion coupling
Baseline	$[(45/-45)_4/0_2]_s$	$[0/(45/-45)_8/(0/90)_6/0]_s$
Positive coupling	$[45_8/0_2]_s$	$[0/45_{16}/(0/90)_6/0]_s$
Negative coupling	$[(-45)_8/0_2]_s$	$[0/(-45)_{16}/(0/90)_6/0]_s$

mining the frequencies, the lag damping was investigated for several different collective pitch angles. At each test condition (collective pitch setting), the lag mode damping was determined using the procedure outlined next.

1) The desired excitation frequency is manually entered into a function generator that controls the swashplate oscillations. The frequency should correspond to the regressing lag frequency obtained earlier (rotor rotational speed − lag frequency = regressing lag frequency).

2) Sinusoidal oscillation of the swashplate is initiated at this frequency. The signal is maintained until the blades reach a sufficient steady-state lag excitation (typically about 1 s).

3) Once a steady-state excitation is reached, data acquisition is initiated and the excitation signal is terminated. The transient response is measured for 10 s at a sampling rate of 256 Hz from strain gauges mounted near the root of the flexbeam. The damping of the desired mode is determined using a moving-block analysis.[17]

4) Steps 1–3 are repeated at least three times for each collective pitch setting.

Theoretical Model

Measurement/Prediction of Flexure Stiffnesses

The stiffnesses of the composite flexbeams were determined experimentally using an optical laser system. Each flexbeam was loaded separately with a tip flap bending load, a tip chordwise bending load, and a tip torque, and the resulting bending slopes (w', v') and twisting deflections (ϕ) were measured at several spanwise locations. The measured values were curve-fit to determine the deflections under a unit tip loading condition. Using these unit deflection values, the effective stiffnesses for each flexbeam were determined from force-displacement relations. For a chordwise bending-torsion coupled composite beam

$$\begin{Bmatrix} M \\ T \end{Bmatrix} = \begin{bmatrix} EI_z & E_{tc} \\ E_{tc} & GJ \end{bmatrix} \begin{Bmatrix} v'' \\ \phi' \end{Bmatrix} \tag{1}$$

where EI_z is the chordwise bending stiffness, GJ is the torsional stiffness, E_{tc} is the bending-torsion structural coupling, v is the chordwise bending, and ϕ is the torsional deflection. M and T represent tip bending and torsion loads, respectively.

Combined with the measured bending slope and twist angles for a chordwise bending-torsion-coupled composite beam, the effective stiffness properties are calculated

$$EI_z = \frac{P_y(Lx - x^2/2)\phi_t}{(v'_p\phi_t - v'_t\phi_p)}, \qquad EI_y = \frac{P_z(Lx - x^2/2)}{w'_p}$$
$$GJ = \frac{Tx v'_p}{(v'_p\phi_t - v'_t\phi_t)}, \qquad E_{tc} = \frac{P_z(Lx - x^2/2)v'_t}{(v'_p\phi_t - v'_t\phi_p)} \tag{2}$$

where w, v, and ϕ are flap bending, lag bending, and twist at the tip of the flexure, respectively, and EI_y is the flap bending stiffness.

Stability Analysis

The comprehensive rotor code, UMARC, is used to perform the aeromechanical stability analysis of a composite hingeless rotor in hover. The rotor blades are modeled as elastic beams undergoing coupled flap bending, lag bending, elastic twist, and axial displacements. The main blade and flexbeam are divided into a number of beam finite elements, each consisting of 15 degrees of freedom. These degrees of freedom correspond to a quadratic variation in elastic twist ϕ; a cubic variation in flap and lag bending deflections w and v, respectively; and a cubic variation in elastic axial deflection u_e. The nonlinear equations governing the behavior are derived, retaining terms up to at least second-order in bending and axial deflection and up to third-order in torsion. The transverse shearing effects are captured implicitly by statically reducing the stiffness matrix.[5]

A rotor aeroelastic stability analysis consists of the calculation of vehicle trim, blade steady response, and stability of the linearized system. For each test condition, the collective pitch θ_0 is specified and the shaft angle α_s is set to 0 deg. The steady blade response determines the blade-deflected position. The nonlinear blade finite element equations are transformed to modal space using natural blade modes and then solved numerically using the finite element in time method. For the shaft-fixed stability analysis, the perturbation equations of motion are linearized about the blade equilibrium position and solved for the stability roots. Again, the equations are transformed to the modal space and solved using an algebraic eigenvalue analysis.

Results and Discussion

Static Tests

Using an optical laser system, the flapwise, lagwise, and torsional stiffnesses of the composite flexures were determined. The stiffness properties obtained from these measurements were used as input into the UMARC stability analysis. Figures 3 and 4 show the agreement between the theoretical predictions and experimentally obtained static response for the chordwise bending-torsion coupled configurations shown in Fig. 2c. Similar agreement was obtained for both the baseline and flapwise bending-torsion coupled cases as well. Table 2 presents the stiffness values calculated from the measured response in both the flapwise bending-torsion and the chordwise bending-torsion coupled configurations. The values were representative of each set of flexbeams tested.

Stability Testing

For the numerical study, a four-bladed soft-in-plane hingeless composite rotor was modeled. The rotor properties are given next. Number of blades = 4, radius = 36.81 in., blade chord = 3 in., blade airfoil = NACA 0012, nominal rotor speed = 900 rpm, solidity $\sigma = 0.1031$, $C_T/\sigma = 0.0488$, precone $\beta_p = 0.0$, lock number $\gamma = 7.78$, and blade pretwist = 0.0 deg. The stability analysis is performed in the rotating frame using a constant coefficient eigensolution. Seven normal modes (three flap, two lag, one torsion, and one axial) are used for the trim analysis, and six modes (three flap, two lag, and one torsion) are used for the stability analysis. Theoretical results are obtained in hover for a collective pitch range from −8 to +8 deg.

By comparing the results of the baseline and coupled configuration flexures, the influence of the composite couplings on rotor stability can be examined. Each coupled flexure was designed to have nearly the same natural frequencies as the corresponding baseline flexure. This would imply that the composite flexures have nearly the same stiffnesses as the baseline flexure, but different elastic couplings. The predicted flap, lag, and torsion frequencies for the different configurations are given in Table 3. The predictions are based upon the measured stiffness properties for each flexbeam model. For all three models, there is only a small difference (within 6%) between the flap and lag frequencies of the baseline and coupled configurations. For both of the composite models, there is a large difference in the torsional frequency predictions between the baseline and the coupled configurations.

Table 2 Measured composite flexure stiffness properties for bending-torsion coupled flexbeams[a]

Stiffness	Baseline flap (mean value) lb/in.^{2}	Coupled flap (mean value) lb/in.^{2}	Coupled chordwise (mean value) lb/in.^{2}
Flap stiffness, EI_y	102	92	4800
Lag stiffness, EI_z	2162	2006	2100
Torsion stiffness, GJ	301	158	800
Flapwise bending-torsion coupling, $E_{\beta\theta}$	——	56	——
Chordwise bending-torsion	——	——	300

[a]L = 6 in.

Table 3 Rotor frequencies at 800 rpm

Flexure	Flap, baseline	Coupled, /rev	Lag, baseline	Coupled, /rev	Torsion, baseline	Coupled, /rev
Isotropic	1.12	——	0.73	——	3.1	——
Pitch-flap composite	1.12	1.12	0.72	0.71	4.4	3.4
Pitch-lag composite	1.17	1.26	0.70	0.724	3.4	5.5

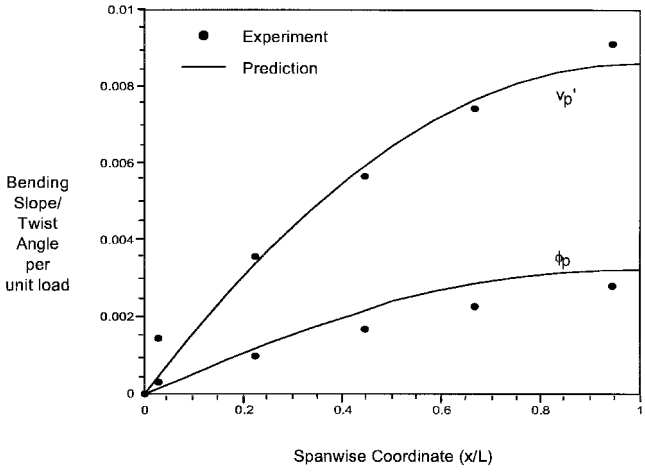

Fig. 3 Lag bending slope and twist angle as a result of unit tip bending load for chordwise bending-torsion-coupled rectangular flexbeam (L = 6 in.).

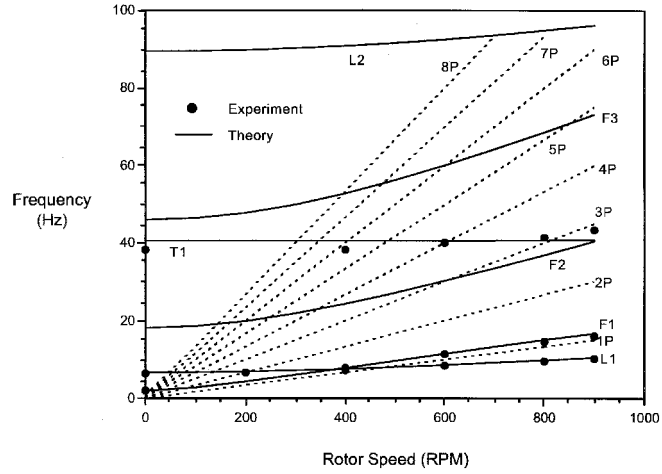

Fig. 5 Fan plot of isotropic Torlon flexure/blade (F = flap, L = lag, T = torsion).

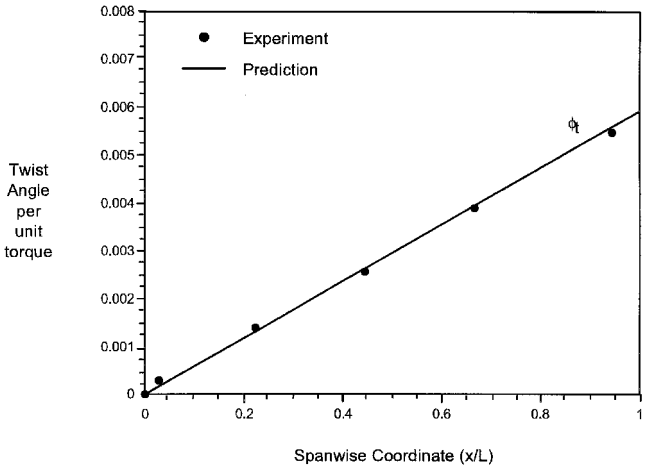

Fig. 4 Twist angle as a result of unit tip torque for chordwise bending-torsion-coupled rectangular flexbeam (L = 6 in.).

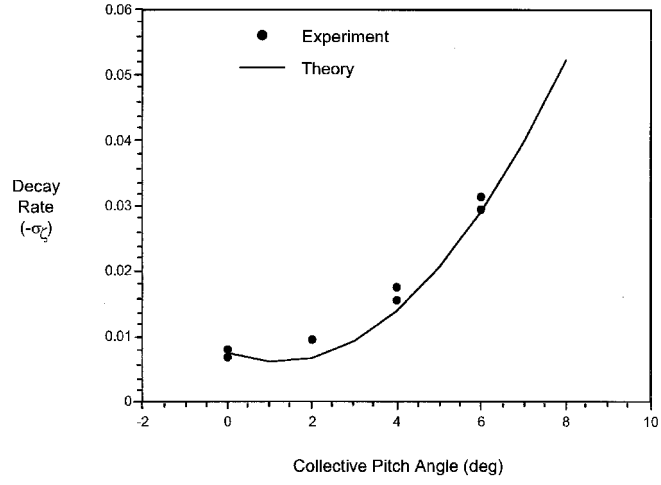

Fig. 6 Lag damping as a function of blade collective pitch angle for baseline isotropic configuration (Ω = 800 rpm).

Isotropic Flexure

In Fig. 5, the natural frequencies of the uncoupled Torlon blade are presented with increasing rotational speed. The experimental data points are shown for the first lag, flap, and torsion modes. Good agreement is seen between theoretical and experimental results for all three modes. Figure 6 shows the lag mode damping in terms of its decay rate (negative of the real part of the stability eigenvalue) vs collective pitch at 800 rpm for the isotropic Torlon flexbeam. Good correlation is seen between experiment and theory over the range of pitch angles. The increase in damping at higher collective pitch angles is attributable to an increase in the aerodynamic coupling.

Flapwise Bending-Torsion Coupling

Figures 7–9 show the comparison between experimentally obtained and predicted values of lag damping at 800 rpm for the flapwise bending-torsion-coupled configurations. Figure 7 shows the lag mode damping in terms of decay rate vs collective pitch for the uncoupled (baseline) configuration. Good correlation is seen between experiment and theoretical predictions over the range of pitch angles. Figure 8 shows the lag damping in terms of its decay rate for the positive flapwise bending-torsion-coupled configuration (flap up–pitch down). Figure 9 shows the lag damping for the negative flapwise bending-torsion-coupled configuration (flap up–pitch up). In Fig. 8 the experimental damping values are underpredicted by the theoretical result (solid line) for positive collective pitch angles. In Fig. 9 good correlation is seen between theoretical and experimental results. The dashed line in both figures represents the theoretical predictions with the coupling term set to zero and all other stiffnesses held fixed. The difference seen between the two lines is caused primarily by frequency differences due to aerodynamic stiffening (δ_3 effect). Over the collective pitch range from -4 to $+4$ degrees, the inclusion of flapwise bending-torsion coupling has only a minor influence on the lag damping as seen in Figs. 8 and 9. The main effect of the introduction of flapwise-bending torsion coupling is to either increase the effective flap frequency (positive coupling) or decrease the effective flap frequency (negative coupling) with only a small influence on lag mode damping.

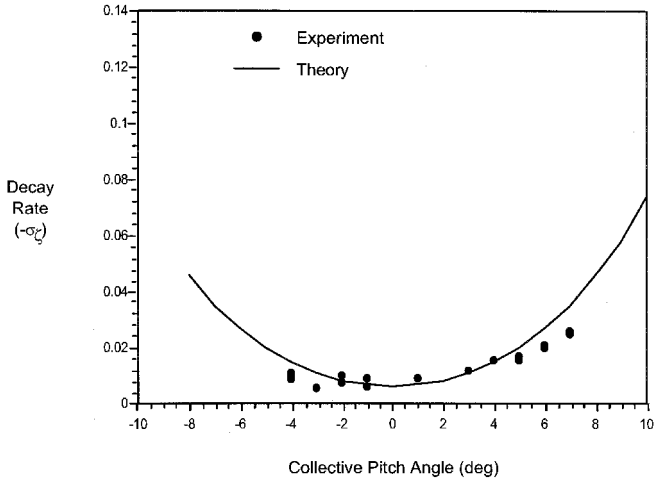

Fig. 7 Lag damping as a function of blade collective pitch angle for baseline (uncoupled) flapwise bending-torsion rectangular configuration (Ω = 800 rpm).

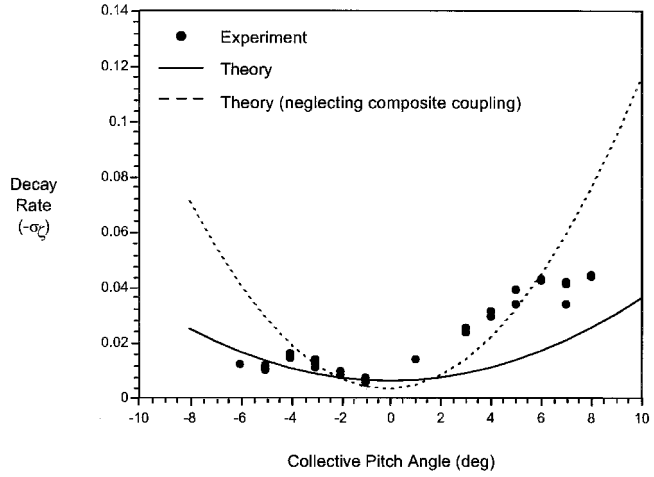

Fig. 8 Lag damping as a function of blade collective pitch angle for positive flapwise bending-torsion-coupled configuration (Ω = 800 rpm).

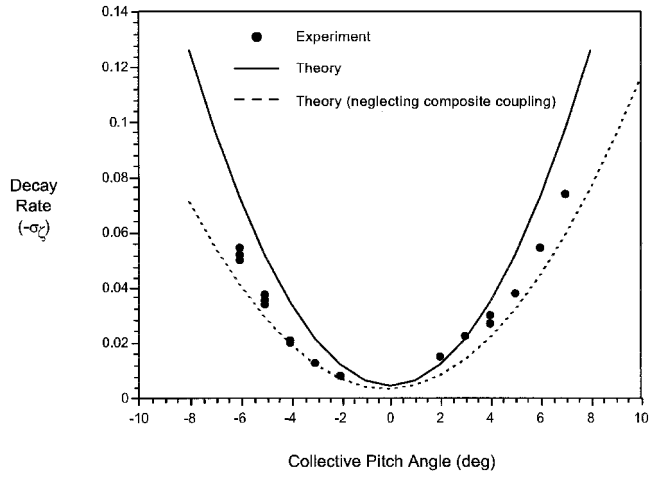

Fig. 9 Lag damping as a function of blade collective pitch angle for negative flapwise bending-torsion-coupled configuration (Ω = 800 rpm).

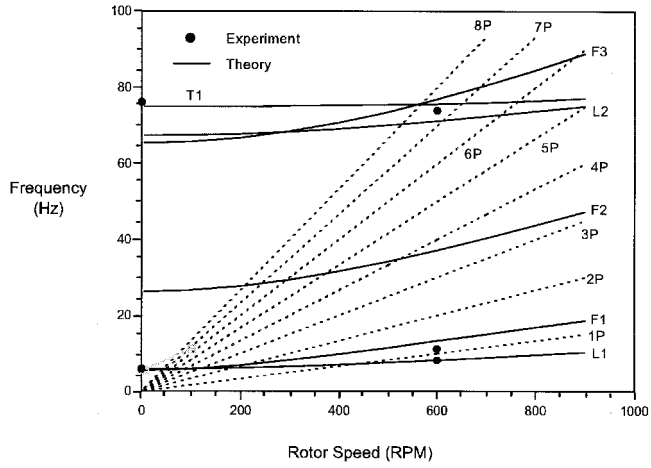

Fig. 10 Fan diagram for chordwise bending-torsion-coupled configuration (F = flap, L = lag, T = torsion).

Chordwise Bending-Torsion Coupling

In Fig. 10, the natural frequencies of the chordwise bending-torsion coupled blade are presented as a function of rotor speed. For both the rotating (600 rpm) and nonrotating test conditions, experimental data points are shown for the first flap, lag, and torsion modes. Figure 11 shows the percent lag mode damping vs collective pitch for the uncoupled (baseline) configuration. Good correlation is seen between experiment and theoretical predictions over the entire range of pitch angles. Figures 12 and 13 show the comparison between experimentally obtained and theoretically predicted values of lag damping at 600 rpm for the chordwise bending-torsion coupled configurations. Figure 12 shows the percent lag damping for the negative chordwise bending-torsion-coupled configuration (lag back–pitch down), whereas Fig. 13 shows the percent lag damping for the positive chordwise bending-torsion-coupled configuration (lag back–pitch up). The dashed line in both figures represent the theoretical predictions with the coupling term set to zero but with all other stiffness properties held fixed. For the negative coupling case, an increase in both theoretical and experimental lag mode damping is seen for increasing positive collective pitch angles relative to the uncoupled configuration. Excellent correlation is seen between the theoretical predictions and experimental data for positive pitch angles. As negative collective pitch increases, the disparity be-

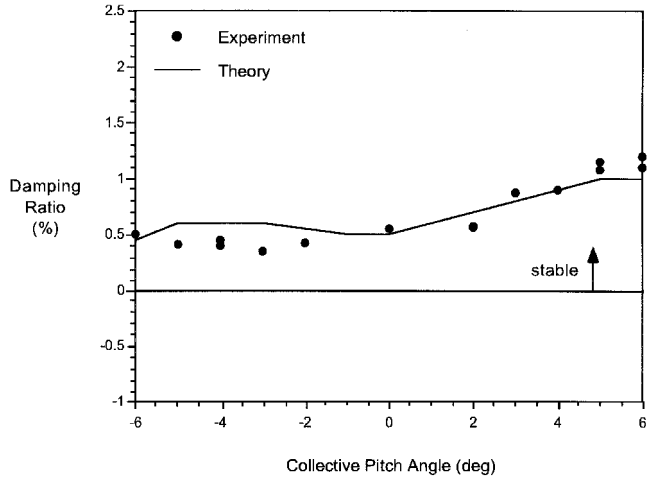

Fig. 11 Lag damping as a function of blade pitch angle for baseline (uncoupled) pitch-lag configuration (Ω = 800 rpm).

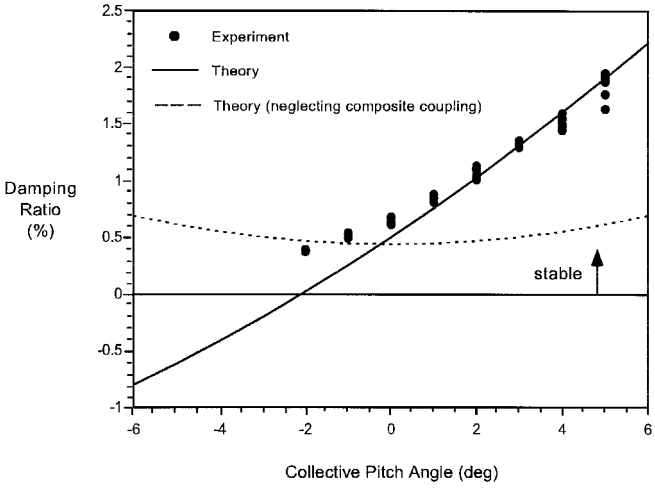

Fig. 12 Lag damping as a function of blade pitch angle for negative pitch-lag-coupled configuration (Ω = 600 rpm).

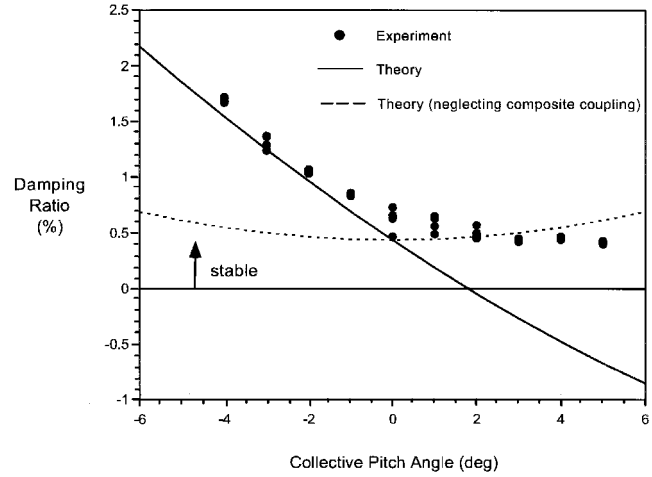

Fig. 13 Lag damping as a function of blade pitch angle for positive pitch-lag-coupled configuration (Ω = 600 rpm).

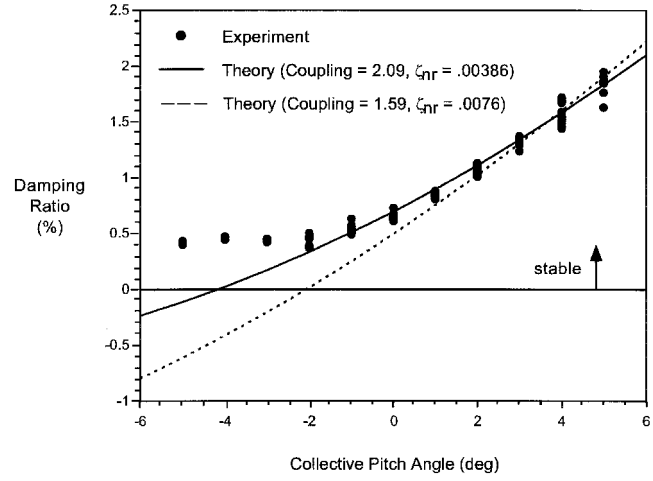

Fig. 14 Lag damping as a function of blade pitch angle for negative pitch-lag-coupled configuration (Ω = 600 rpm).

tween theoretical and experimental values becomes larger. Experimentally, the influence of negative chordwise bending-torsion coupling diminishes for negative collective pitch angles. For the positive chordwise bending-torsion coupling configuration, trends opposite those in the negative coupling configuration are seen. The lag mode damping is increased for negative collective pitch angles and exhibits excellent correlation between experimental values and theoretical predictions. The influence of positive chordwise bending-torsion coupling diminishes for positive collective pitch angles.

Disparity between the coupling stiffness and the structural damping may be the cause of the discrepancy between the theoretical predictions and experimental results for negative collective pitch angles in the negative-coupled configuration and for positive pitch angles in the positive-coupled configuration. For both configurations the coupling stiffness used in the theoretical predictions (shown in Figs. 12 and 13) corresponds to the statically obtained nondimensional value of 2.09 (300 lb in.^{2}), whereas the structural damping parameter used was 0.00386. Parametric studies were performed to investigate the influence of the coupling stiffness magnitude and the structural lag damping value and the results were presented previously.[18] For example, for the negative pitch-lag-coupled configuration, a 25% decrease in elastic coupling combined with an increase in structural lag damping improves the correlation for the negative collective pitch angles (Fig. 14).

Conclusions

A systematic investigation of the aeroelastic stability of a composite hingeless rotor has been performed. Four different composite flexbeams were designed, built, and tested. Correlation studies with UMARC are performed. The following conclusions were drawn based upon this investigation:

1) For the baseline isotropic Torlon case, good correlation between theoretical predictions and experimental results are shown.

2) For the composite flexure cases, elastic flapwise bending-torsion (pitch-flap) coupling has only a small effect on the lag damping.

3) Elastic chordwise bending-torsion (pitch-lag) coupling has a powerful influence on the lag damping of a hingeless rotor. Negative chordwise bending-torsion coupling has a strong stabilizing effect on the lag damping for increasing positive collective pitch angles. The lag damping is destabilized for positive collective pitch angles with the introduction of positive chordwise bending-torsion coupling.

4) From hover testing, it is shown using elastically tailored composite flexures can have a powerful influence on the aeroelastic stability of a hingeless rotor.

Acknowledgments

This research work is supported by the U.S. Army Reseach Office under the Center for Rotorcraft Education and Research, Grant DAAH-04-94-G-0074. The Technical Monitor was Tom

Doligalski. The authors also thank Gene Joo for his technical contributions to this research.

References

[1]Hong, C. H., and Chopra, I., "Aeroelastic Stability Analysis of a Composite Blade," *Journal of the American Helicopter Society*, Vol. 30, No. 2, 1985, pp. 57–67.

[2]Panda, B., and Chopra, I., "Dynamics of Composite Rotor Blades in Forward Flight," *Vertica*, Vol. 11, No. 1/2, 1987, pp. 107–209.

[3]Smith, E. C., and Chopra, I., "Aeroelastic Response, Loads, and Stability of a Composite Rotor in Forward Flight," *AIAA Journal*, Vol. 31, No. 7, 1993, pp. 1265–1273.

[4]Smith, E. C., and Chopra, I., "Air and Ground Resonance of Helicopters with Elastically Tailored Composite Rotor Blades," *Journal of the American Helicopter Society*, Vol. 38, No. 4, 1993, pp. 50–61.

[5]Tracy, A. L., and Chopra, I., "Aeromechanical Stability of a Composite Bearingless Rotor in Forward Flight," *Proceedings of the AIAA/AHS/ASME/ASCE/ASC 34th Structures, Structural Dynamics, and Materials Conference* (La Jolla, CA), AIAA, Washington, DC, 1993.

[6]Tracy, A. L., and Chopra, I., "Aeroelastic Analysis of a Composite Bearingless Rotor in Forward Flight Using an Improved Warping Model," *Journal of the American Helicopter Society*, Vol. 40, No. 3, 1995, pp. 80–91.

[7]Yuan, K., Friedmann, P. P., and Venkatesan, C., "A New Aeroelastic Model for Composite Rotor Blades with Straight and Swept Tips," *Proceedings of the AIAA/AHS/ASME/ASCE/ASC 33rd Structures, Structural Dynamics, and Materials Conference* (Dallas, TX), AIAA, Washington, DC, 1992.

[8]Fulton, M. V., and Hodges, D. H., "Aeroelastic Stability of Composite Hingeless Rotor Blades in Hover—Part I: Theory," *Mathematical and Computer Modelling*, Vol. 18, No. 3/4, 1993, pp. 1–18.

[9]Fulton, M. V., and Hodges, D. H., "Aeroelastic Stability of Composite Hingeless Rotor Blades in Hover—Part II: Results," *Mathematical and Computer Modelling*, Vol. 18, No. 3/4, 1993, pp. 19–35.

[10]Bousman, W. G., Sharpe, D. L., and Ormiston, R. A., "An Experimental Study of Techniques for Increasing the Lead-Lag Damping of Soft Inplane Hingeless Rotors," *Proceeding of the 32nd AHS Annual National V/STOL Forum*, American Helicopter Society, Alexandria, VA, 1976, pp. 1–12.

[11]Bousman, W. G., "An Experimental Investigation of the Effects of Aeroelastic Couplings on Aeromechanical Stability of a Hingeless Rotor Helicopter," *Journal of the American Helicopter Society*, Vol. 26, No. 1, 1981, pp. 46–54.

[12]Bousman, W. G., "The Effects of Structural Flap-Lag and Pitch-Lag Coupling on Soft Inplane Hingeless Rotor Stability in Hover," NASA TP 3002, AVSCOM TR89-A-002, May 1990.

[13]Yeager, W. T., Hamouda, M. H., and Mantany, W. R., "An Experimental Investigation of the Aeromechanical Stability of a Hingeless Rotor in Hover and Forward Flight," NASA TM 89107, AVSCOM TM 87-B-5, June 1987.

[14]McNulty, M. J., "Flap-Lag Stability Data for a Small-Scale Isolated Hingeless Rotor in Forward Flight," NASA TM 102189, AVSCOM TR 89-A-003, April 1989.

[15]Sharpe, D. L., "An Experimental Investigation of the Flap-Lag-Torsion Aeroelastic Stability of the Small-Scaled Hingeless Helicopter Rotor in Hover," NASA TP2546, AVSCOM TR 85-A-9, Jan. 1986.

[16]Maier, T. H., Sharpe, D. L., and Lim, J. W., "Fundamental Investigation of Hingeless Rotor Aeroelastic Stability, Test and Correlation," *Proceedings of the 51st American Helicopter Society Annual Forum* (Fort Worth, TX), American Helicopter Society, Alexandria, VA, 1995, pp. 1176–1190.

[17]Tasker, F. A., and Chopra, I., "Assessment of Transient Analysis Techniques for Rotor Stability Testing," *Journal of the American Helicopter Society*, Vol. 35, No. 1, 1990, pp. 39–50.

[18]Tracy, A. L., "Aeromechanical Stability Investigation of Elastically Coupled Composite Helicopter Rotors," Ph.D. Dissertation, Dept. of Aerospace Engineering, Univ. of Maryland, College Park, MD, 1996.